On the second-order temperature jump coefficient of a dilute gas

AUTHOR(S):

Radtke, Gregg A.; Hadjiconstantinou, N. G.; Takata, S.; Aoki, K.

CITATION:

Radtke, Gregg A. ...[et al]. On the second-order temperature jump coefficient of a dilute gas. Journal of Fluid Mechanics 2012, 707: 331-341

ISSUE DATE:

2012-09

URL:

http://hdl.handle.net/2433/193962

J. Fluid Mech. (2012), *vol.* 707, *pp.* 331–341.
doi:10.1017/jfm.2012.282

On the second-order temperature jump coefficient of a dilute gas

Gregg A. Radtke[1], N. G. Hadjiconstantinou[1]†, S. Takata[2] and K. Aoki[2]

[1] Department of Mechanical Engineering, Massachusetts Institute of Technology, Cambridge, MA 02139, USA

[2] Department of Mechanical Engineering and Science, Kyoto University, Kyoto 606-8501, Japan

(Received 17 October 2011; revised 4 March 2012; accepted 9 June 2012; first published online 20 July 2012)

We use LVDSMC (low-variance deviational Monte Carlo) simulations to calculate, under linearized conditions, the second-order temperature jump coefficient for a dilute gas whose temperature is governed by the Poisson equation with a constant forcing term, as in the case of homogeneous volumetric heating. Both the hard-sphere gas and the BGK model of the Boltzmann equation, for which slip/jump coefficients are not functions of temperature, are considered. The temperature jump relation and jump coefficient determined here are closely linked to the general jump relations for time-dependent problems that have yet to be systematically treated in the literature; as a result, they are different from those corresponding to the well-known linear and steady case where the temperature is governed by the homogeneous heat conduction (Laplace) equation.

Key words: kinetic theory, MEMS/NEMS, non-continuum effects

1. Introduction

Slip-flow theory is a powerful tool that enables the continued use of the Navier–Stokes description as the characteristic flow length scale (L) approaches the molecular mean free path (λ) (Beskok & Karniadakis 2002). It can be rigorously derived from an asymptotic solution of the Boltzmann equation in the limit $Kn = \lambda/L \ll 1$; such an analysis shows that, in this limit, the Navier–Stokes description remains valid in the bulk, but fails near the boundaries (Sone 2002, 2007). Fortunately, the kinetic effects associated with the inhomogeneity introduced by the walls are only important within a layer of thickness $O(\lambda)$ near the boundaries (known as the Knudsen layer) and can be accounted for by a boundary-layer type of analysis where an inner kinetic solution is matched to the outer Navier–Stokes solution (Sone 2002, 2007). Slip/jump boundary conditions and the associated non-adjustable slip coefficients emerge from this analysis as the matching condition between the inner and outer solution (Sone 2002, 2007). Carrying out such an analysis to second order in Kn yields models that are generally expected to improve the accuracy of first-order

† Email address for correspondence: ngh@mit.edu

slip-corrected Navier–Stokes solutions, and in many cases allow use of the Navier–Stokes description in the early transition regime ($0.1 \lesssim Kn \lesssim 0.4$), provided the existence of Knudsen layers in the vicinity of the boundaries, which cannot be captured by the Navier–Stokes description, is accounted for (Hadjiconstantinou 2006).

Accurate determination of slip coefficients using this rigorous procedure is quite challenging in general and becomes increasingly more challenging as the order of the expansion increases. Original studies focused on the BGK model of the Boltzmann equation (Cercignani 1962; Sone 1969, 1971), for which all first-order and second-order coefficients are known (Sone 2002, 2007). The first-order coefficients for the hard-sphere gas have also since been calculated (Ohwada, Sone & Aoki 1989*a*,*b*; Sone, Ohwada & Aoki 1989). However, although the form of the slip expression is known to second order in Kn, second-order slip coefficients for the hard-sphere gas are mostly unknown.

As a companion paper (Takata *et al.* 2012) shows, the reciprocity relations recently developed by Takata (2009, 2010) can be used to calculate these coefficients. Alternatively, slip coefficients can be obtained from hydrodynamic fields by comparing the Boltzmann equation with Navier–Stokes solutions (Hadjiconstantinou 2003, 2006). In these approaches, in addition to high accuracy (including low statistical uncertainty if a stochastic method is used for solving the Boltzmann equation), care needs to be exercised to avoid comparison of the two solutions in the Knudsen layer, where the Navier–Stokes solution is not equivalent to the Boltzmann solution (Hadjiconstantinou 2006).

In this paper we use this process to calculate the second-order temperature jump coefficient for a dilute gas when the temperature field is governed by the Poisson equation with constant forcing term; as shown in the companion paper and further discussed below, our results are closely related to the second-order slip/jump description of time-dependent problems. Here, we calculate jump coefficients using the low-variance deviational Monte Carlo (LVDSMC) method (Homolle & Hadjiconstantinou 2007*a*,*b*; Radtke & Hadjiconstantinou 2009; Radtke, Hadjiconstantinou & Wagner 2011), which is naturally suited to low-signal problems and thus allows calculations at infinitesimal temperature differences. The latter are necessary because finite temperature variations may alter the result through density gradients or the temperature dependence of transport coefficients.

In the following section we review temperature jump boundary conditions for steady problems. In § 3 we describe the problem formulation that allows us to extract the new temperature jump coefficient. In § 4 we describe the computational method and in § 5 we present our simulation results. We close with a discussion of the significance of our results and ways in which they can be generalized.

2. Background

We consider a dilute hard-sphere gas of molecular mass m and molecular diameter σ, in contact with a planar diffusely reflecting boundary at temperature T_B. We also consider the BGK model of such a gas, with collision frequency τ^{-1}. In the case of the hard-sphere gas, $\lambda = (\sqrt{2}\pi n_0 \sigma^2)^{-1}$, while for the BGK gas $\lambda = 2c_0\tau/\sqrt{\pi}$, where $c_0 = \sqrt{2RT_0}$ is the most probable speed based on the reference temperature T_0, n_0 is a reference number density, $R = k_B/m$ is the gas constant and k_B is Boltzmann's constant.

Although the theory discussed here is valid for flowing gases, in the interest of simplicity, we limit our discussion to flows that are quiescent under no-slip boundary

conditions. The additional terms introduced in the temperature jump conditions by flow stresses are known for steady problems and can be found in Sone (2002).

The first-order temperature jump condition at the gas–wall interface is given by

$$\hat{T}|_B - \hat{T}_B = d_1 k \left.\frac{\partial \hat{T}}{\partial \hat{n}}\right|_B, \tag{2.1}$$

where $\hat{T} = T/T_0 - 1$, $k = (\sqrt{\pi}/2)Kn = (\sqrt{\pi}/2)(\lambda/L)$, $|_B$ denotes the boundary location, $\hat{n}$ is the unit (inward) normal direction and L is the characteristic system length scale; the numerical constant d_1 has the non-adjustable values of 2.4001 for a hard-sphere gas and 1.30272 for a BGK gas (Sone 2002) for diffusely reflecting boundaries.

The first-order result (2.1) is typically adequate for $Kn < 0.1$. Asymptotic expansion to second order in k (Sone 2002, 2007) for linear and steady problems extends (2.1) to

$$\hat{T}|_B - \hat{T}_B = (d_1 + d_5 \bar{\kappa} k) k \left.\frac{\partial \hat{T}}{\partial \hat{n}}\right|_B + d_3 k^2 \left.\frac{\partial^2 \hat{T}}{\partial \hat{n}^2}\right|_B. \tag{2.2}$$

Here $\bar{\kappa}/L$ is the mean boundary curvature and $d_5 = 1.82181$ for the BGK model (Sone 2002); for the hard-sphere gas the value of d_5 is unknown. We emphasize that according to the analysis that yields this condition, for linear and steady problems, energy conservation reduces to

$$\nabla^2 \hat{T} = \frac{\partial^2 \hat{T}}{\partial \hat{x}^2} + \frac{\partial^2 \hat{T}}{\partial \hat{y}^2} + \frac{\partial^2 \hat{T}}{\partial \hat{z}^2} = 0, \tag{2.3}$$

where $(\hat{x}, \hat{y}, \hat{z}) = (x/L, y/L, z/L)$. In the special case of one-dimensional problems, (2.3) further reduces to

$$\nabla^2 \hat{T} = \frac{\mathrm{d}^2 \hat{T}}{\mathrm{d}\hat{n}^2} = 0, \tag{2.4}$$

which makes the value of d_3 irrelevant. This is utilized below to calculate the jump coefficient due to a forcing term in the temperature equation.

In summary, jump condition (2.2) is to be used when the governing equation is (2.3). Within this approximation, d_3 is only known ($d_3 = 0$) for the special case of the BGK model (Sone 2002, 2007). We also note that Deissler's result (Deissler 1964) for second-order velocity slip and temperature jump is based on approximate mean-free-path arguments and does not correspond to a self-consistent solution of the Boltzmann equation; as a result, it captures neither the correct form of the slip/jump relation nor the correct values of the slip coefficients (e.g. compare (3.40)–(3.42) in Sone (2007) to (24*a*) and (51) in Deissler (1964)).

3. Calculation of the temperature jump coefficient

To extract the jump coefficient in a dilute gas governed by the Poisson equation with constant forcing term, we simulate the steady state of a one-dimensional gas layer bounded by two isothermal, diffuse walls at $x = \pm L/2$ and at temperature T_0, subject to volumetric heating at a constant rate $\dot{Q}$; a discussion of the kinetic-level formulation of this problem can be found in the next section. In dimensionless form, the one-dimensional heat equation with constant volumetric heating can be written as

$$\nabla^2 \hat{T} = \frac{\mathrm{d}^2 \hat{T}}{\mathrm{d}\hat{x}^2} = -\frac{5\epsilon}{4\gamma_2 k}, \tag{3.1}$$

where γ_2 is a dimensionless form of the thermal conductivity equal to 1.92228 for hard spheres and unity for BGK (Sone 2007), and

$$\epsilon = \frac{L\dot{Q}}{c_0 P_0} \ll 1 \tag{3.2}$$

is the dimensionless form of the volumetric heat addition rate. Here, $P_0 = n_0 k_B T_0$ is a reference pressure.

The asymptotic analysis yielding (2.2) does not apply to the non-homogeneous equation (3.1). A rigorous derivation which takes the inhomogeneous term into account by considering an equivalent unsteady problem can be found in the companion paper (Takata *et al.* 2012), which shows that in a quiescent gas, in one spatial dimension, the resulting second-order slip relation is given by

$$\hat{T}|_B - \hat{T}_B = d_1 k \left.\frac{\partial \hat{T}}{\partial \hat{n}}\right|_B + d_3' k^2 \left.\frac{\partial^2 \hat{T}}{\partial \hat{n}^2}\right|_B . \tag{3.3}$$

We emphasize that, although the structure of the slip relation is the same as in (2.2), the second-order coefficient is different. It is also convenient that (3.3) does not contain d_3; this allows calculation of d_3' from volumetric heating calculations without explicit knowledge of d_3. This last feature, as well as the similarity of (2.2) and (3.3) is due to fortuitous cancellation; as discussed further in § 6, under more general conditions (e.g. higher spatial dimensions), this cancellation does not take place and terms containing both d_3 and d_3' appear.

The solution to (3.1) subject to boundary condition (3.3) is

$$\hat{T} = \frac{1}{2}\frac{4\epsilon}{5\gamma_2 k}\left[\left(\frac{1}{4} - \hat{x}^2\right) + d_1 k - 2 d_3' k^2\right]. \tag{3.4}$$

Comparison of this solution to LVDSMC simulations away from the Knudsen layer allows us to calculate the coefficient d_3'. Here, we extract the value of d_3' from the slope of

$$\frac{5\gamma_2}{4\epsilon}\hat{T}(\hat{x}=0) - \frac{1}{8k} - \frac{d_1}{2} \tag{3.5}$$

as a function of k for $k \to 0$.

4. Computational method

The low-variance deviational simulation Monte Carlo (LVDSMC) method (Homolle & Hadjiconstantinou 2007*a*,*b*; Radtke & Hadjiconstantinou 2009; Hadjiconstantinou, Radtke & Baker 2010; Radtke *et al.* 2011) efficiently simulates (Wagner 2008) the Boltzmann equation

$$\frac{\partial f}{\partial t} + \boldsymbol{c}\cdot\frac{\partial f}{\partial \boldsymbol{x}} = \left[\frac{\partial f}{\partial t}\right]_{coll} \tag{4.1}$$

written here in the absence of external body forces, by simulating only the deviation ($f^d = f - f^{MB}$) from an equilibrium state f^{MB}. Here, $f = f(\boldsymbol{x}, \boldsymbol{c}, t)$ is the single-particle distribution function (Sone 2002) and

$$f^{MB} = \frac{\rho_{MB}}{\pi^{3/2} c_{MB}^3}\exp\left(-\frac{\|\boldsymbol{c} - \boldsymbol{u}_{MB}\|^2}{c_{MB}^2}\right), \tag{4.2}$$

based on local (cell-based) mass density ρ_{MB}, velocity $\boldsymbol{u}_{MB}$, temperature T_{MB}, and most probable velocity $c_{MB} = \sqrt{2RT_{MB}}$. Because f^d can take positive and negative values, it is represented by signed deviational particles. Deviational methods exhibit greatly reduced statistical uncertainty for low-signal problems compared to the standard DSMC (Bird 1994) approach and are therefore well suited to the present application.

Volumetric heating is modelled by simulating the augmented Boltzmann equation

$$\frac{\partial f}{\partial t} + \boldsymbol{c} \cdot \frac{\partial f}{\partial \boldsymbol{x}} = \left[\frac{\partial f}{\partial t}\right]_{coll} + \frac{\dot{Q}}{P_0}\left(\frac{2}{3}\frac{c^2}{c_0^2} - 1\right) f^0, \tag{4.3}$$

where $f^0 = \rho_0 \left(\sqrt{\pi} c_0\right)^{-3} \exp[-\|\boldsymbol{c}\|^2 / c_0^2]$ and $\rho_0 = m n_0$. Here we note that the heat generation term – that directly leads to the source term in (3.1) – is not unique, in the sense that, in general, different source terms are expected to yield different jump conditions. The one used here was chosen because it naturally lends itself to a physical interpretation in terms of the time-dependent problem studied in the companion paper (Takata *et al.* 2012). This also serves to explain the connection between our results and the general theory of high-order slip/jump in time-dependent problems.

As in DSMC, LVDSMC solves the Boltzmann transport equation through time-splitting using a time step Δt. Although different derivations are possible, here we take $f^{MB} \neq f^{MB}(t)$, as originally proposed (Homolle & Hadjiconstantinou 2007*b*) and theoretically analysed (Wagner 2008). In other words, and as also further discussed in § 4.2, although ρ_{MB}, $\boldsymbol{u}_{MB}$ and T_{MB} vary during the simulation, their variation is attributed to a 'quasi-static change of basis' that occurs once every time step and not an explicit time dependence of f^{MB}. The resulting advection and collision substeps are described below.

4.1. *Advection substep*

Substituting $f = f^d + f^{MB}$ into the left-hand side of (4.1) with $f^{MB} \neq f^{MB}(t)$, yields

$$\frac{\partial f^d}{\partial t} + \boldsymbol{c} \cdot \frac{\partial f^d}{\partial \boldsymbol{x}} = -\boldsymbol{c} \cdot \frac{\partial f^{MB}}{\partial \boldsymbol{x}}. \tag{4.4}$$

This implies that the advection step in LVDSMC can be treated by collisionless advection of deviational particles (solution of the homogeneous equation) plus a correction due to the spatial variation of f^{MB} (particular solution). In the LVDSMC methods used here, f^{MB} is either constant throughout the computational domain, or piece-wise constant in each cell. In the former case no particular solution is required, while in the latter case the solution can be shown (Homolle & Hadjiconstantinou 2007*b*) to require particle generation at the cell boundaries. Generated particles are sampled from the distribution

$$\boldsymbol{c} \cdot \boldsymbol{n} \left(f_-^{MB} - f_+^{MB}\right) \Delta A^{int} \Delta t \, \mathrm{d}^3\boldsymbol{c}, \tag{4.5}$$

where ΔA^{int} is the area of the interface, $f_\pm^{MB}$ are the equilibrium distributions in adjacent cells, and $\boldsymbol{n}$ points from f_-^{MB} to f_+^{MB}. Particles are generated every time step and advected for a random fraction of the time step, after which they become part of the deviational particle population.

A stationary domain boundary is a special case of the above solution where a discontinuity is formed between the distribution imposed by the boundary and the f^{MB} of the cell adjacent to it. In this case particles need to be generated from the

distribution

$$\boldsymbol{c}\cdot\boldsymbol{n}\left(\rho_B\phi^B - f^{MB}\right)\Delta A\Delta t\,\mathrm{d}^3\boldsymbol{c}, \tag{4.6}$$

where ΔA is the surface area element at the boundary, f^{MB} is the equilibrium distribution in the cell adjacent to the boundary, and $\phi^B = (\pi c_B^2)^{-3/2}\exp[-c^2/c_B^2]$ is the 'boundary distribution', where the $c_B = \sqrt{2RT_B}$; the 'boundary density' ρ_B is evaluated from the mass conservation statement (Radtke & Hadjiconstantinou 2009)

$$\rho_B\int_{\boldsymbol{c}\cdot\boldsymbol{n}>0}\boldsymbol{c}\cdot\boldsymbol{n}\,\phi^B\,\mathrm{d}^3\boldsymbol{c} = -\int_{\boldsymbol{c}\cdot\boldsymbol{n}<0}\boldsymbol{c}\cdot\boldsymbol{n}\,f^{MB}\,\mathrm{d}^3\boldsymbol{c}. \tag{4.7}$$

4.2. *Collision substep*

The collision substep treatment is based on published LVDSMC implementations (Radtke & Hadjiconstantinou 2009; Radtke *et al.* 2011), suitably modified to include the effect of volumetric heating. We first discuss the BGK collision operator and the corresponding volumetric heating implementation; the hard-sphere case follows. Owing to the small deviations from equilibrium, here we consider the linearized form of these operators; methods for simulating the corresponding nonlinear versions can be found in Homolle & Hadjiconstantinou (2007*b*), Wagner (2008) and Hadjiconstantinou *et al.* (2010).

4.2.1. *BGK model*

In the case of the BGK model, the collision operator is given by

$$\left[\frac{\partial f}{\partial t}\right]_{coll} = -\frac{f - f^{loc}}{\tau}, \tag{4.8}$$

where f^{loc} is the local equilibrium distribution given by

$$f^{loc} = \frac{\rho(\boldsymbol{x},t)}{[2\pi RT(\boldsymbol{x},t)]^{3/2}}\exp\left(-\frac{\|\boldsymbol{c}-\boldsymbol{u}(\boldsymbol{x},t)\|^2}{2RT(\boldsymbol{x},t)}\right), \tag{4.9}$$

and $\rho(\boldsymbol{x},t)$, $\boldsymbol{u}(\boldsymbol{x},t)$ and $T(\boldsymbol{x},t)$ are the local density, flow velocity and temperature.

By adding and subtracting the term Δf^{MB}, the equation governing the collision substep can be written (Radtke & Hadjiconstantinou 2009) as

$$\left[\frac{\partial f}{\partial t}\right]_{coll}\Delta t = \underbrace{\frac{\Delta t}{\tau}\left[f^{loc} - f^{MB}\right] - \Delta f^{MB}}_{\text{generation}} + \underbrace{\Delta f^{MB}}_{\text{shift in } f^{MB}} - \underbrace{\frac{\Delta t}{\tau}f^d}_{\text{deletion}}, \tag{4.10}$$

which can be decomposed into a source term for new particles, a shift in the equilibrium state and a sink term for deleting existing particles. As discussed above, the shift term effects a 'change of basis' in which the previous equilibrium distribution (f^{MB}) is replaced by a new equilibrium distribution ($f^{MB} + \Delta f^{MB}$), while particles sampling $-\Delta f^{MB}$ are generated and added to f^d ($f = f^{MB} + \Delta f^{MB} - \Delta f^{MB} + f^d$). Although, in principle, this update happens after the collision substep, in the interest of efficiency and in order to maximize particle cancellation (see below), this update is integrated into, and happens simultaneously with, the collision substep.

It can be shown (Radtke & Hadjiconstantinou 2009) that when the equilibrium state (for each cell) is updated according to

$$\begin{bmatrix} \rho_{MB} \\ \boldsymbol{u}_{MB} \\ T_{MB} \end{bmatrix} (t+\Delta t) = \begin{bmatrix} \rho_{MB} \\ \boldsymbol{u}_{MB} \\ T_{MB} \end{bmatrix} (t) + \frac{\Delta t}{\tau} \begin{bmatrix} \rho - \rho_{MB} \\ \boldsymbol{u} - \boldsymbol{u}_{MB} \\ T - T_{MB} \end{bmatrix} (t) \tag{4.11}$$

cancellation between $f^{loc} - f^{MB}$ and Δf^{MB} causes the generation term to vanish. This is in agreement with the physical interpretation of the collision operator in the relaxation-time approximation, namely that collisions drive the distribution towards the local equilibrium. This is exploited here to significantly simplify step (4.10).

The same change-of-basis argument can be used to treat the heat generation term

$$\dot{Q} = \rho_0 \frac{\mathrm{d}}{\mathrm{d}t} \left(\frac{3}{2} R T_{MB} \right), \tag{4.12}$$

resulting in the following update (every time step) for the temperature parameter of the equilibrium distribution:

$$\Delta T_{MB} = \frac{2\dot{Q}\Delta t}{3\rho_0 R}. \tag{4.13}$$

4.2.2. *Hard-sphere model*

The hard-sphere collision operator can be written as

$$\left[\frac{\partial f^d}{\partial t} \right]_{coll} = \underbrace{\int \left[2K^{(1)} - K^{(2)} \right] (\boldsymbol{c}, \boldsymbol{c}_*) f(\boldsymbol{c}_*) \, \mathrm{d}^3 \boldsymbol{c}_*}_{\text{generation}} - \underbrace{\nu(\boldsymbol{c}) f(\boldsymbol{c})}_{\text{deletion}} \tag{4.14}$$

allowing the collision step to be processed as a series of Markov particle generation and deletion steps as proposed by Wagner (2008); the specific algorithms employed are discussed in detail in Wagner (2008) and Radtke *et al.* (2011). Denoting $\xi = \|\boldsymbol{c} - \boldsymbol{u}_{MB}\| / c_{MB}$ we obtain

$$K^{(1)}(\boldsymbol{c}, \boldsymbol{c}_*) = \frac{\sigma^2 \rho_{MB}}{\sqrt{\pi} m c_{MB} \|\boldsymbol{c} - \boldsymbol{c}_*\|} \exp\left(- \frac{[(\boldsymbol{c} - \boldsymbol{u}_{MB}) \cdot (\boldsymbol{c} - \boldsymbol{c}_*)]^2}{c_{MB}^2 \|\boldsymbol{c} - \boldsymbol{c}_*\|^2} \right), \tag{4.15}$$

$$K^{(2)}(\boldsymbol{c}, \boldsymbol{c}_*) = \frac{\pi \sigma^2}{m} \|\boldsymbol{c} - \boldsymbol{c}_*\| f^{MB}(\boldsymbol{c}), \tag{4.16}$$

$$\nu(\boldsymbol{c}) = \frac{\pi \sigma^2 \rho_{MB} c_{MB}}{m} \left[\frac{\exp(-\xi^2)}{\sqrt{\pi}} + \left(\xi + \frac{1}{2\xi} \right) \operatorname{erf}(\xi) \right]. \tag{4.17}$$

Unlike the BGK case, f^{MB} is not updated every time step because the hard-sphere simulation algorithm used here is based (Radtke 2011; Radtke *et al.* 2011) on the fixed global equilibrium distribution f^0. However, to improve accuracy for the low values of Kn considered here, we have developed an algorithm which uses an equilibrium distribution (f^{MB}) that is spatially dependent (but not updated every time step). (As shown in Radtke & Hadjiconstantinou 2009, LVDSMC methods with a variable equilibrium distribution significantly outperform their counterparts with a fixed equilibrium distribution in the limit $Kn \to 0$, because they are able to track the local equilibrium distribution and thus minimize the number of particles required for the

same solution fidelity.) Similarly to the BGK case, the objective of this algorithm is to make $f^{MB} \approx f^{loc}$; in the present case this is achieved using an iterative algorithm in which ρ_{MB} and T_{MB} are taken from the solution at the previous iteration, while the velocity $\boldsymbol{u}_{MB}$ is taken to be zero. This process is started with $f^{MB} = f^0$ and iterated until f^{MB} no longer changes appreciably, which usually takes less than 2 iterations.

Since the heat generation term on the right-hand side of (4.3) represents the rate of change of the distribution function due to the uniform heat generation, the latter is implemented by generating particles from the distribution

$$\left[\frac{\partial f^d}{\partial t}\right]_{heat} = \frac{\dot{Q}}{P_0}\left(\frac{2}{3}\frac{c^2}{c_0^2} - 1\right) f^0. \tag{4.18}$$

The number of computational particles (of both signs) generated per unit time is given by the integral of the absolute value of this expression over all molecular velocities and the volume of interest, divided by the effective number (the number of deviational particles simulated by each computational particle). Since the generation is uniform in space, particles can be uniformly generated throughout the simulation domain. Algorithms for efficiently sampling distributions of the form (4.18) are described in Radtke & Hadjiconstantinou (2009), Radtke *et al.* (2011) and Radtke (2011).

5. Results

Following extensive numerical experiments, simulations of uniform heat generation were performed using a cell size $\Delta x \leqslant \lambda/10$ and a time step $\Delta t \leqslant \Delta x/2c_0$. Hard-sphere simulations were performed using a number of particles per cell that ranged from approximately 1300 for $Kn = 0.1$ to approximately 2600 for $Kn = 0.04$. Owing to their significantly smaller cost, BGK simulations were performed with more than 10 000 particles per cell.

The second-order jump coefficients are determined by comparing the simulated centreline temperature $\hat{T}(\hat{x} = 0)$ with the prediction of (3.4) at $\hat{x} = 0$. Figure 1 shows our numerical data for $-kd_3'$ and a linear least-squares fit passing through the origin based on the data for $k < 0.06$, and the values $d_1 = 1.30272$ for BGK and $d_1 = 2.4001$ for the hard-sphere gas (Sone 2007). These fits yield $d_3' = -1.4$ for BGK and -3.1 for the hard-sphere model; the fit quality demonstrates that the leading-order term in (3.5) is indeed proportional to k. The contribution of higher-order terms starts to be noticeable as k increases. Incidentally, the complementary analysis of the companion paper, based on a finite-difference analysis of the Knudsen-layer problem of the linearized Boltzmann equation, yields $d_3' = -1.4276$ for the BGK model and $d_3' = -3.180$ for the hard-sphere model.

The disparity between the temperature jump coefficients of the two gases is in part due to the difference in their thermal conductivities (γ_2). If we account for the difference in thermal conductivity (e.g. by taking $k_{BGK} = 1.92228 k_{HS}$ leading to 'effective' jump coefficients $1.92228 d_1$ and $1.92228^2 d_3'$ for the BGK model) the first-order and second-order coefficients of the two gases differ by approximately 5 % and 66 %, respectively.

Figure 2(*a*) shows the temperature field for the hard-sphere case with $Kn = 0.05$ (equivalent to $k = 0.0443$) using the value obtained above (namely $d_3' = -3.1$), demonstrating excellent agreement everywhere except in the Knudsen layer close to the boundary, as expected. By comparing the first- and second-order jump theories, it is clear that at $Kn = 0.05$ the second-order jump theory already provides an improvement over the existing first-order theory. For $Kn = 0.1$ (figure 2*b*), the error in

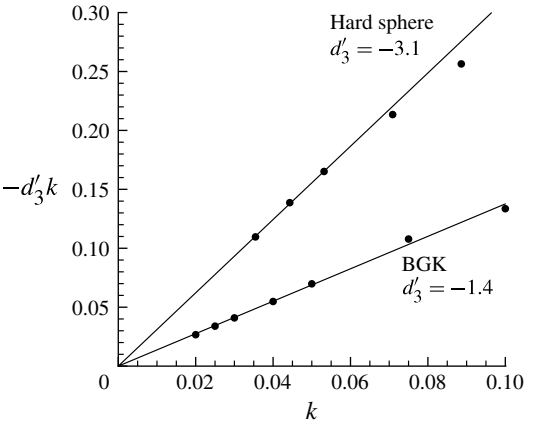

FIGURE 1. Fits used to extract the second-order jump coefficient d_3'.

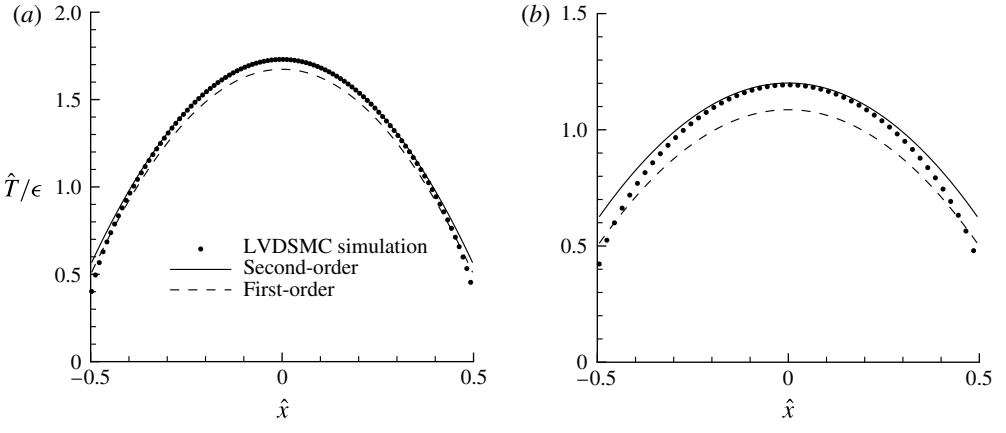

FIGURE 2. LVDSMC simulation results (symbols) are compared to the first-order (dashed line) and second-order (solid line) jump theories ((3.4) with $d_3' = 0$ and $d_3' = -3.1$, respectively): (*a*) $Kn = 0.05$; (*b*) $Kn = 0.1$.

the first-order solution is quite large, while the second-order solution is considerably more accurate, provided we recall that Knudsen layers adjacent to the walls and extending a few mean free paths (recall that $x/\lambda = \hat{x}/Kn$) into the domain prevent the slip/jump-corrected Navier–Stokes solution from matching the Boltzmann (LVDSMC) solution there.

6. Discussion

Using LVDSMC simulations, we have extracted the second-order temperature jump coefficient for a hard-sphere and a BGK gas in the case that the Navier–Stokes-limit behaviour is captured by an inhomogeneous heat conduction equation, such as the one appearing in the presence of constant volumetric heating. Our results have been validated and put on a more firm theoretical footing by a companion paper which provides a deterministic calculation of the same coefficient through a rigorous

asymptotic analysis of the Boltzmann equation of a mathematically equivalent problem, namely that of a quiescent gas confined between two parallel walls whose temperature increases/decreases linearly in time at a constant (and small) rate. Owing to the time-dependent nature of the latter problem, the analysis in the companion paper goes beyond the asymptotic theory for steady problems (Sone 2002); this explains why the jump coefficient (d_3') calculated here is not equivalent to the one (d_3) appropriate for steady problems.

Equations (3.1) and (3.3) can be generalized to two- and three-dimensional steady problems as long as the heat generation is uniform in space and constant in time. Specifically, for a quiescent gas, the governing equation and boundary condition in this case become

$$\nabla^2 \hat{T} = -\frac{5\epsilon}{4\gamma_2 k} \tag{6.1}$$

and

$$\hat{T}|_B - \hat{T}_B = (d_1 + d_5\bar{\kappa}k)k\frac{\partial \hat{T}}{\partial \hat{n}}\bigg|_B + d_3' k^2 \frac{\partial^2 \hat{T}}{\partial \hat{n}^2}\bigg|_B + (d_3' - d_3)k^2\left(\nabla^2 \hat{T} - \frac{\partial^2 \hat{T}}{\partial \hat{n}^2}\right)\bigg|_B, \tag{6.2}$$

respectively. As explained in § 1, in the presence of gas flow, additional terms related to the flow stress appear in (6.2). These terms can be found in Sone (2002).

More generally, d_3' is one of a set of unknown coefficients that extend the steady, asymptotic theory of Sone (2002) – valid for $Kn \ll 1$ and $Ma \ll Re \ll 1$, where Ma and Re are the Mach and Reynolds number, respectively – to unsteady phenomena in the same limit. A complete discussion can be found in Takata & Hattori (2012). Problems beyond the range of validity of such asymptotic theories (e.g. $Kn \not\ll 1$, moderately/highly curved boundaries) or characterized by complex multidimensional geometries can be treated by direct numerical solutions or simulations of the Boltzmann equation (e.g. LVDSMC).

Acknowledgements

This work was supported in part by the Singapore–MIT Alliance. N.G.H. would like to thank K.A. for his hospitality during his visit to Kyoto University in 2010. The authors would also like to thank the Mechanical Engineering Department at MIT for supporting the visit of K.A. through a Peabody Visiting Professorship.

REFERENCES

Beskok, A. & Karniadakis, G. 2002 *Microflows: Fundamentals and Simulation*. Springer.

Bird, G. A. 1994 *Molecular Gas Dynamics and the Direct Simulation of Gas Flows*. Oxford Science.

Cercignani, C. 1962 Elementary solutions of the linearized gasdynamics Boltzmann equation and their application to the slip-flow problem. *Ann. Phys.* **20**, 219.

Deissler, R. G. 1964 An analysis of second-order slip flow and temperature-jump boundary conditions for rarefied gases. *Intl J. Heat Mass Transfer* **7**, 681–694.

Hadjiconstantinou, N. G. 2003 Comment on Cercignani's second-order slip coefficient. *Phys. Fluids* **15**, 2352–2354.

Hadjiconstantinou, N. G. 2006 The limits of Navier–Stokes theory and kinetic extensions for describing small-scale gaseous hydrodynamics. *Phys. Fluids* **18** (11), 111301.

HADJICONSTANTINOU, N. G., RADTKE, G. A. & BAKER, L. L. 2010 On variance-reduced simulations of the Boltzmann transport equation for small-scale heat transfer applications. *Trans. ASME: J. Heat Transfer* **132**, 112401.

HOMOLLE, T. M. M. & HADJICONSTANTINOU, N. G. 2007*a* Low-variance deviational simulation Monte Carlo. *Phys. Fluids* **19**, 041701.

HOMOLLE, T. M. M. & HADJICONSTANTINOU, N. G. 2007*b* A low-variance deviational simulation Monte Carlo for the Boltzmann equation. *J. Comput. Phys.* **226**, 2341–2358.

OHWADA, T., SONE, Y. & AOKI, K. 1989*a* Numerical analysis of the Poiseuille and thermal transpiration flows between parallel plates on the basis of the Boltzmann equation for hard-sphere molecules. *Phys. Fluids* A **1**, 2042.

OHWADA, T., SONE, Y. & AOKI, K. 1989*b* Numerical analysis of the shear and thermal creep flows of a rarefied gas over a plane wall on the basis of the linearized Boltzmann equation for hard-sphere molecules. *Phys. Fluids* A **1**, 1588.

RADTKE, G. A. 2011 Efficient simulation of molecular gas transport for micro- and nanoscale applications. PhD thesis, Massachusetts Institute of Technology.

RADTKE, G. A. & HADJICONSTANTINOU, N. G. 2009 Variance-reduced particle simulation of the Boltzmann transport equation in the relaxation-time approximation. *Phys. Rev.* E **79** (5), 056711.

RADTKE, G. A., HADJICONSTANTINOU, N. G. & WAGNER, W. 2011 Low-noise Monte Carlo simulation of the variable hard-sphere gas. *Phys. Fluids* **23**, 030606.

SONE, Y. 1969 Asymptotic theory of flow of rarefied gas over a smooth boundary I. In *Sixth Intl Symp. on Rarefied Gas Dynamics* (ed. L. Trilling & H. Y. Wachman). *Rarefied Gas Dynamics*, vol. 1, pp. 243–253. Academic.

SONE, Y. 1971 Asymptotic theory of flow of rarefied gas over a smooth boundary II. In *Seventh Intl. Symp. on Rarefied Gas Dynamics* (ed. D. Dini). *Rarefied Gas Dynamics*, vol. 2, pp. 737–749. Editrice Tecnico Scientifica.

SONE, Y. 2002 *Kinetic Theory and Fluid Dynamics*. Birkhäuser.

SONE, Y. 2007 *Molecular Gas Dynamics: Theory, Techniques, and Applications*. Birkhäuser.

SONE, Y., OHWADA, T. & AOKI, K. 1989 Temperature jump and Knudsen layer in a rarefied gas over a plane wall: Numerical analysis of the linearized Boltzmann equation for hard-sphere molecules. *Phys. Fluids* A **1**, 363.

TAKATA, S. 2009 Symmetry of the linearized Boltzmann equation and its application. *J. Stat. Phys* **136**, 751.

TAKATA, S. 2010 Symmetry of the unsteady linearized Boltzmann equation in a fixed bounded domain. *J. Stat. Phys.* **140**, 985.

TAKATA, S., AOKI, K., HATTORI, M. & HADJICONSTANTINOU, N. G. 2012 Parabolic temperature profile and second-order temperature jump of a slightly rarefied gas in an unsteady two-surface problem. *Phys. Fluids* **24**, 032002.

TAKATA, S. & HATTORI, M. 2012 Asymptotic theory for the time-dependent behaviour of a slightly rarefied gas over a smooth solid boundary. *J. Stat. Phys.* **147**, 1182.

WAGNER, W. 2008 Deviational particle Monte Carlo for the Boltzmann equation. *Monte Carlo Meth. Appl.* **14**, 191–268.